Investigation of properties limiting efficiency in -based solar cells

Investigation of Properties Limiting Efficiency in $Cu_2ZnSnSe_4$-Based Solar Cells

Guy Brammertz, Souhaib Oueslati, Marie Buffière, Jonas Bekaert, Hossam El Anzeery, Khaled Ben Messaoud, Sylvester Sahayaraj, Thomas Nuytten, Christine Köble, Marc Meuris, and Jozef Poortmans

***Abstract*—We have investigated different nonidealities in $Cu_2ZnSnSe_4$–CdS–ZnO solar cells with 9.7% conversion efficiency, in order to determine what is limiting the efficiency of these devices. Several nonidealities could be observed. A barrier of about 300 meV is present for electron flow at the absorber–buffer heterojunction leading to a strong crossover behavior between dark and illuminated current–voltage curves. In addition, a barrier of about 130 meV is present at the Mo–absorber contact, which could be reduced to 15 meV by inclusion of a TiN interlayer. Admittance spectroscopy results on the devices with the TiN backside contact show a defect level with an activation energy of 170 meV. Using all parameters extracted by the different characterization methods for simulations of the two-diode model including injection and recombination currents, we come to the conclusion that our devices are limited by the large recombination current in the depletion region. Potential fluctuations are present in the devices as well, but they do not seem to have a special degrading effect on the devices, besides a probable reduction in minority carrier lifetime through enhanced recombination through the band tail defects.**

Manuscript received June 30, 2014; revised October 23, 2014; accepted November 20, 2014.

G. Brammertz, S. Sahayaraj, and M. Meuris are with the IMEC Division IMOMEC—partner in Solliance, 3590 Diepenbeek, Belgium, and also with the Institute for Material Research (IMO), Hasselt University, 3590 Diepenbeek, Belgium (e-mail: brammert@imec.be; sahaya@imec.be; meuris@imec.be).

S. Oueslati is with the IMEC Division IMOMEC—partner in Solliance, 3590 Diepenbeek, Belgium, with the Institute for Material Research (IMO), Hasselt University, 3590 Diepenbeek, Belgium, with the KACST-Intel Consortium Center of Excellence in Nano-manufacturing Applications, Riyadh, KSA, and with the Faculty of Sciences of Tunis, University of Tunis El Manar, 2092 Tunis, Tunisia (e-mail: oueslati@imec.be.).

M. Buffiere is with IMEC, 3001 Leuven, Belgium, and also with the Department of Electrical Engineering, Katholieke Universiteit Leuven, 3001 Heverlee, Belgium (e-mail: buffiere@imec.be).

J. Bekaert is with the Department of Physics, University of Antwerp, 2020 Antwerpen, Belgium (e-mail: Jonas.Bekaert@uantwerpen.be).

H. El Anzeery is with the IMEC Division IMOMEC—partner in Solliance, 3590 Diepenbeek, Belgium, with the Institute for Material Research (IMO), Hasselt University, 3590 Diepenbeek, Belgium, with the KACST-Intel Consortium Center of Excellence in Nano-manufacturing Applications, Riyadh, KSA, and with the Microelectronics System Design Department, Nile University, Cairo, Egypt (e-mail: hossam@imec.be).

K. Ben Messaoud is with the IMEC Division IMOMEC—partner in Solliance, 3590 Diepenbeek, Belgium, with the Institute for Material Research (IMO), Hasselt University, 3590 Diepenbeek, Belgium, with the KACST-Intel Consortium Center of Excellence in Nano-manufacturing Applications, Riyadh, KSA, and with the Faculty of Sciences of Tunis, University of Tunis El Manar, 2092 Tunis, Tunisia (e-mail: messaoud@imec.be).

T. Nuytten is with the IMEC, 3001 Leuven, Belgium (e-mail: nuytte30@imec.be).

C. Köble is with the Helmholtz-Zentrum Berlin für Materialien und Energie GmbH, 14109 Berlin, Germany (e-mail: koeble@helmholtz-berlin.de).

J. Poortmans is with IMEC, 3001 Leuven, Belgium, and also with the Department of Electrical Engineering, Katholieke Universiteit Leuven, 3001 Heverlee, Belgium (e-mail: poortman@imec.be).

Color versions of one or more of the figures in this paper are available online at http://ieeexplore.ieee.org.

Digital Object Identifier 10.1109/JPHOTOV.2014.2376053

***Index Terms*—Admittance spectroscopy, $Cu_2ZnSnSe_4$ (CZTSe), defect, kesterite, solar cell.**

I. Introduction

THIN-FILM chalcogenide photovoltaics seem to be a promising alternative to further reduce the cost of solar energy in the future. Whereas CdTe- and $Cu(In,Ga)(S,Se)_2$-based technologies are already well established in the solar module market, $Cu_2ZnSn(S,Se)_4$ (CZTSSe) kesterite-based solar cells are currently being investigated as an alternative chalcogenide absorber material with high constituent element abundance [1], [2]. Recent results have shown a conversion efficiency as high as 12.6% with a hydrazine solution processed $Cu_2ZnSn(S,Se)_4$ absorber in combination with a CdS buffer layer [3]. Despite the good results achieved, further improvements in the conversion efficiency are necessary in order to be able to compete with the already much higher efficiencies achieved with CdTe and $Cu(In,Ga)(S,Se)_2$ technologies [4]. In the present contribution, we analyze the optoelectrical properties of $Cu_2ZnSnSe_4$ (CZTSe)-based solar cells with a total area conversion efficiency of 9.7% [5]. From the optoelectrical characterization, we will try to determine which nonideality in the devices is actually limiting the conversion efficiency by comparing the experimental results to a two-diode model simulation using all the parameters extracted from the electrooptical characterization.

II. Sample Fabrication and Physical Characterization

Our CZTSe solar cells are fabricated by selenization of sequentially sputtered metal precursors [6]. First, $Cu_{10}Sn_{90}$, Zn, and Cu metal layers are sputtered on to a standard Mo on soda lime glass substrate. The stacked metal layers are then selenized in a rapid thermal anneal oven in vacuum, where a continuous flow of 10% H_2Se in N_2 is supplied. The ramp up speed is 1 °C/s, the anneal time is fixed at 15 min, and the anneal temperature is fixed at about 450 °C. The temperature is measured on the backside of the susceptor, whereas heating is through lamp heating to the front side of the sample; therefore, actual temperature on the sample front side could be higher than the measured 450 °C. A KCN etch is then performed followed by chemical bath deposition of 50 nm of CdS and sputtering of 120 nm of intrinsic ZnO, followed by sputter deposition of 250 nm of Al-doped ZnO. A Ni/Al top contact grid is then deposited, and cell isolation is made with needle scribing. Finally, a 110-nm-thick MgF_2 antireflective coating layer is deposited. A top-view scanning electron microscopy (SEM) picture of a typical absorber layer is shown in Fig. 1(a), whereas Fig. 1(b) shows a cross-sectional SEM of a

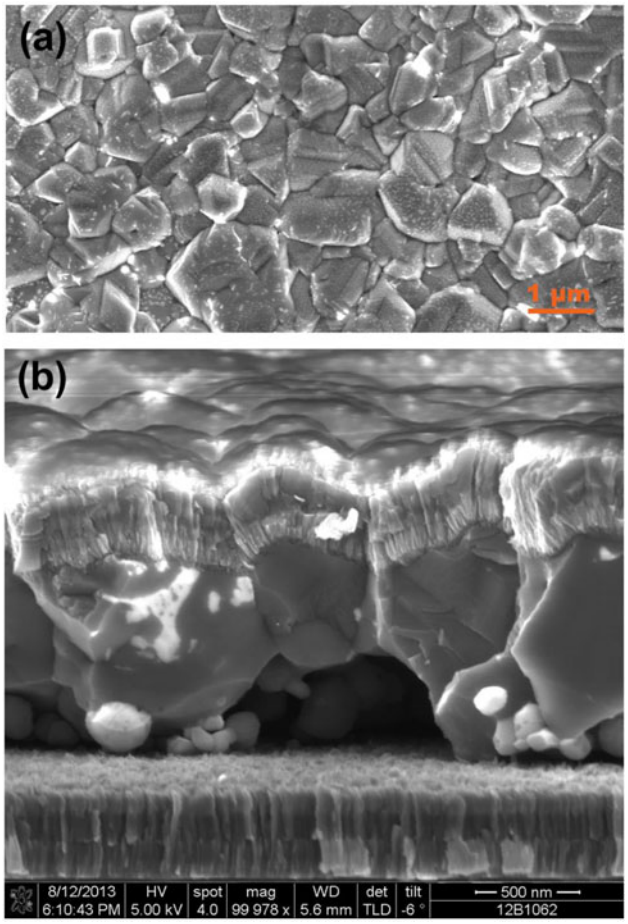

Fig. 1. (a) SEM image of a typical absorber layer after selenization. (b) Cross-sectional SEM image of the highest efficiency solar cell device.

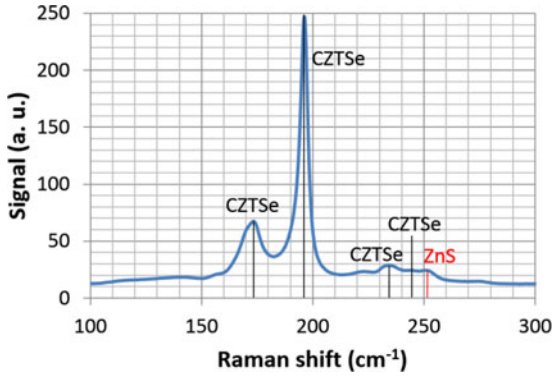

Fig. 2. Raman spectrum of the highest efficiency CZTSe absorber layer.

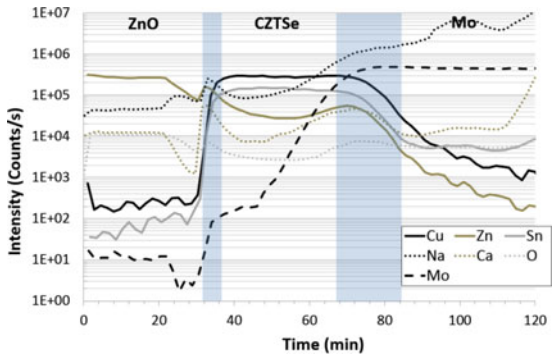

Fig. 3. Secondary ion mass spectroscopy measurement on a CZTSe-CdS-ZnO solar cell sample. The shaded regions represent the approximate interfaces between the different materials.

finished solar cell device. Typical grain sizes of about 1 μm diameter are visible, as well as some amount of secondary phases with typically much smaller grain size. The average composition of the absorber layer, as measured from energy dispersive X-ray spectroscopy, was determined as Cu/(Zn + Sn) = 0.7, Zn/Sn = 1, and Se/(Cu + Zn + Sn) = 1.08. The sample is, therefore, very Cu-poor, stoichiometric with respect to Zn and Sn, and quite Se-rich. A Raman spectrum of our highest efficiency solar cell is shown in Fig. 2. Raman measurements were performed using a Horiba Jobin-Yvon LabRAM HR confocal spectrometer with 50 $\times$ 0.55 NA objective and 8 μW of laser excitation light at 633 nm. Multiple spectra on different locations across the sample were averaged to obtain a representative Raman characterization of the layer. The variations from spot to spot were very limited such that the presented graph is very representative of the overall Raman behavior. Besides the main peaks generally attributed to CZTSe at 173, 196, 234, and 243 nm^{-1} [7], a peak at 251 nm^{-1} can be clearly identified, suggesting the presence of a considerable amount of ZnSe in the absorber [8]. Secondary ion mass spectroscopy analysis on a similar solar cell sample is shown in Fig. 3. Whereas the Cu and Sn concentrations are relatively homogeneous throughout the thickness of the absorber layer, the Zn seems to be present in higher concentrations at the front and back interfaces. Large diffusion of Na and Ca from the soda lime glass substrate into the absorber layer is visible, as well as the presence of a nonnegligible amount of oxygen. From the mass spectroscopy profile, it seems that the front interface is better defined than the back interface, which is also confirmed by the cross-sectional SEM images, which are showing large holes at the backside of the sample. Diffusion of Cu and Zn into the top ZnO layer is very limited.

III. Electrooptical Characterization

Dark and illuminated current–voltage measurements of the best 1-cm^2 solar cell device are shown in Fig. 4. The total area conversion efficiency using a standard AM1.5G spectrum with an illumination intensity of 1000 W/m^2 is 9.7%. A very strong crossover point between the dark and the illuminated curves can be identified in the figure. This crossover is possibly due to a light-dependent barrier of about 300 meV between the CZTSe absorber layer and the CdS buffer layer, which can be very strongly reduced using light illumination with an energy above the CdS bandgap [9]. Under AM1.5G illumination, this barrier, therefore, does not seem to affect the operation of the device, whereas in the dark, it adds an additional series resistance.

CZTSe solar cells present an increasing series resistance as the temperature is reduced to cryogenic temperatures [10]. It was shown through variation of the backside contact metal that

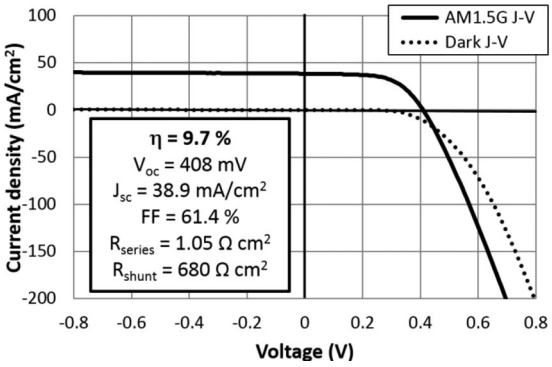

Fig. 4. Dark and illuminated current–voltage measurement of the highest efficiency 1-cm^2 solar cell together with the performance metrics.

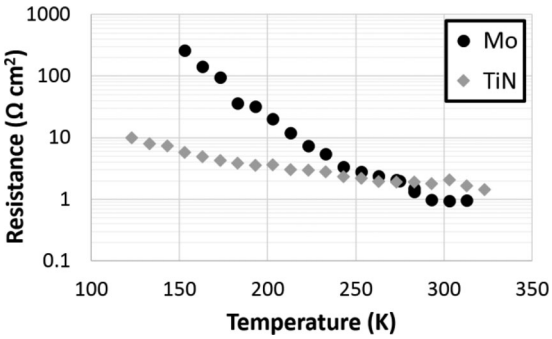

Fig. 5. Series resistance as a function of temperature for two similar devices: one with a standard Mo backside contact and the other one with a 100-nm-thick TiN layer introduced between the Mo and the absorber.

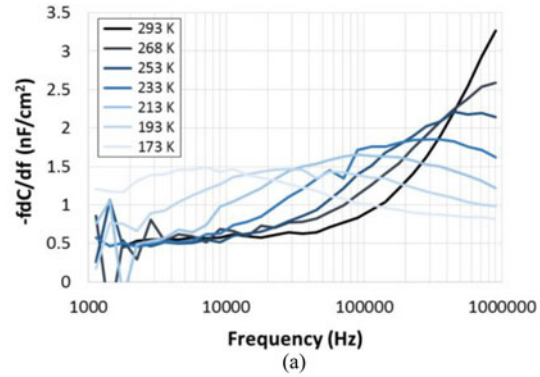

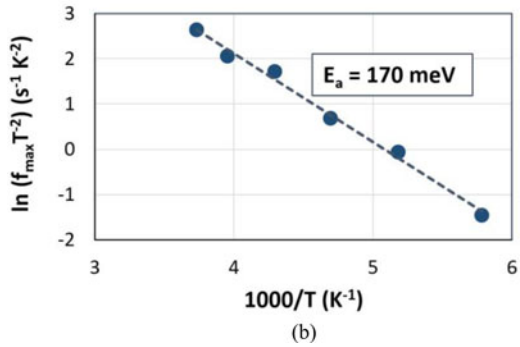

Fig. 6. (a) *–fdC/df* as a function of measurement frequency for different temperatures. (b) Arrhenius plot of the peak maximum frequency.

this behavior was related to a backside contact barrier [11]. The barrier height derived for a Mo backside contact is of the order of 130 meV [10], [5]. Even though such a barrier only adds a few tenths of $\Omega \cdot \text{cm}^2$ at room temperatures, it was shown that, through the deposition of a 100-nm-thick sputtered TiN layer on top of the Mo, the barrier could be reduced to 15 meV, reducing the contact resistance due to this effect basically to zero. In addition, the strong increase in the series resistance at lower temperatures could be avoided, as becomes visible from Fig. 5. Fig. 5 shows a plot of the series resistance as a function of temperature for a device with Mo backside contact and the same device including a 100-nm-thick TiN layer between the Mo and the absorber layer. As the large series resistance also gives a trace in admittance spectroscopy measurements [12], it has, to date, been difficult to reliably study the defect density in the absorber with this type of measurements. For the devices with the TiN barrier layer, this problem is no more present, and admittance measurements can be acquired without the complication of the rising series resistance. Fig. 6(a) shows the admittance response of a CZTSe–CdS–ZnO solar cell device with similar processing as compared with our highest efficiency devices, but with an additional TiN layer between the Mo and the absorber. The efficiency of this device is 8.5%, with no antireflective coating deposited and, therefore, very similar efficiency, as compared with the best device presented here [11]. A clear peak can be identified in the derivative of the capacitance response at the different measurement temperatures and the peak shifts to lower frequencies as the temperature is reduced. An Arrhenius plot of the frequency of the maximum of the peak [13] is shown in Fig. 6(b), from which a main defect with an activation energy of 170 meV can be derived. No other peak can be seen in the admittance response, which is the reason why we believe that no deeper defect is present. Nevertheless, the peaks in *–fdC/df* do not return to zero, but rather seem to stabilize at a value of 0.5 nF/cm^2. Therefore, it could be that in addition to the main defect level at 170 meV, a certain continuous background of defect states is present in the material.

Fig. 7(a) shows the internal quantum efficiency (IQE) of the device with the highest efficiency as a function of applied bias voltage. Good carrier collection can be seen with large IQE in excess of 90% in the range 500–900 nm. Increasing the reverse bias voltage only increases carrier collection by a small amount, but when the device is forward biased, the carrier collection degrades considerably already for small bias voltages. By fitting a simple model for the IQE to the experimental bias-dependent data, it has been shown that for every wavelength, the absorption coefficient and the diffusion length can be derived [14], [15]. The necessary relationship between bias voltage and depletion layer width is derived from capacitance versus voltage measurements. We have applied this method here, and the results for the absorption coefficient as a function of wavelength are shown in Fig. 7(b). The diffusion length derived from the fitting is equal to 2 ± 0.5 μm.

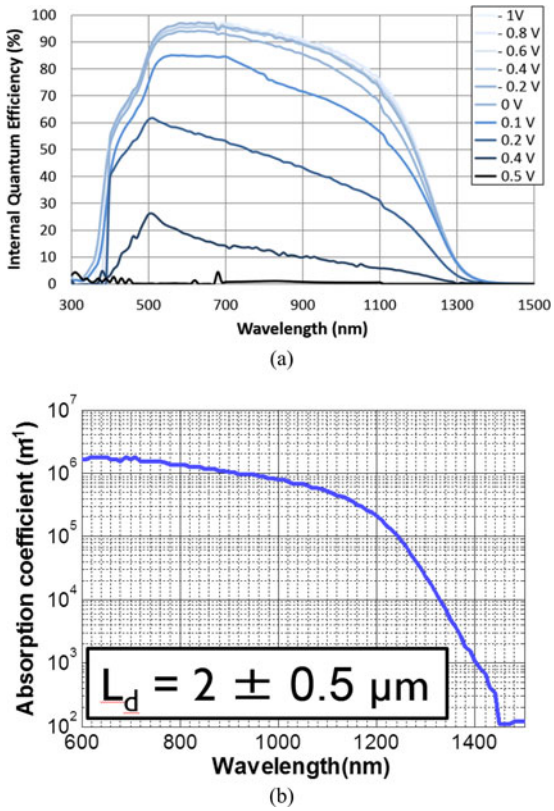

Fig. 7. (a) IQE of the CZTSe–CdS–ZnO solar cell as a function of applied bias voltage. (b) Absorption coefficient as a function of illumination wavelength derived from fitting the bias dependent IQE. The value of the derived wavelength independent minority carrier diffusion length L_d is shown as well.

IV. Two-Diode Simulation

The current density under illumination through a n^+-p diode can be written as [16] follows:

$$J = J_{\rm sc} - J_{0,1}\left[\exp\left(\frac{qV}{kT}\right) - 1\right] - J_{0,2}\left[\exp\left(\frac{qV}{2kT}\right) - 1\right] \quad (1)$$

where

$$J_{0,1} = \frac{qL_d n_i^2}{\tau N_A} \text{ and } J_{0,2} = \frac{qWn_i}{2\tau}. \quad (2)$$

Here, $J_{0,1}$ and $J_{0,2}$ are the reverse saturation currents, $J_{\rm sc}$ is the short-circuit current density, L_d is the minority carrier diffusion length, τ is the minority carrier lifetime, n_i is the intrinsic carrier density, and W is the depletion layer width. The first term in (1) accounts for the currents originating from the neutral regions of the junction, whereas the second term accounts for currents generated through carrier generation–recombination in the depletion region of the junction.

In (2), the intrinsic carrier density n_i is given by

$$n_i = \sqrt{N_C N_V}\exp\left(\frac{-E_g}{2kT}\right) \quad (3)$$

with

$$N_x = 2\left(\frac{2\pi m_x kT}{h^2}\right)^{3/2}. \quad (4)$$

TABLE I
Parameters for Two-Diode Model Simulations

Symbol	Name	Unit	Values
$J_{\rm sc}$	Short-circuit current density	mA/cm^2	38.9
E_g	Bandgap	eV	0.97
m_C	Effective mass of electrons	/	0.1
m_V	Effective mass of holes	/	0.4
N_A	Acceptor density	cm^{-3}	2×10^{15}
τ	Minority carrier lifetime	ns	7
L_d	Diffusion length	μm	2
ε_r	Relative permittivity	/	8
ψ_{bi}	Built-in potential	eV	0.9
R_s	Series resistance	$\Omega \cdot$cm^2	1.05
$R_{\rm shunt}$	Shunt resistance	$\Omega \cdot$cm^2	680

Here, $x = C$ or V; N_C and N_V are the effective density of states in the conduction and valence band, respectively; E_g is the bandgap; m_C and m_V are the average effective masses of electrons and holes, respectively; and *k* and *h* are the Boltzmann and Planck constants, respectively. The depletion layer width *W* is given by

$$W = \sqrt{\frac{2\varepsilon_r\varepsilon_0\left(\psi_{bi} - V\right)}{qN_A}} \quad (5)$$

where $\varepsilon_{\rm r}$ is the relative permittivity, and $\psi_{\rm bi}$ is the built-in field in the junction.

We know or can estimate quite well all of the parameters that are necessary for calculating (1). Table I summarizes the values that we used. The bandgap was derived from the absorption edge of the IQE curve, the average effective masses of electrons and holes were taken from [17], the acceptor density and minority carrier lifetime in the absorber were measured [5], the minority carrier diffusion length was derived from the bias dependence of the IQE, the relative permittivity was taken from [18], the built-in potential was estimated as being slightly below the bandgap value, and the series and shunt resistance values were derived directly from the *J–V* curves of Fig. 4. Using all these parameters for calculating the *J–V* curve in (1), including the effect of the series and shunt resistance, we obtain a good fit to the experimental device results, as can be seen in Fig. 8(a).

The calculated values for the reverse saturation currents $J_{0,1}$ and $J_{0,2}$ were 10^{-10} and 10^{-5} A $\cdot$ cm^{-2}, respectively. Our best device, therefore, seems to be strongly limited by $J_{0,2}$, i.e., the recombination current in the depletion region, due to a combination of low bandgap, large width of the depletion region, and a relatively low minority carrier lifetime, in agreement with other studies on kesterite solar cells [3], [10], [14], [18], [19]. This conclusion can also be confirmed by a plot of the open-circuit voltage as a function of cell efficiency for a larger range of fabricated CZTSe solar cells. All cells were fabricated with a process flow similar to the one described above but with variations in the different metal layer thickness and anneal times and temperatures. The solid line represents the open-circuit voltage calculated using (1) and the parameters from Table I, varying only the value of the minority carrier lifetime. The experimental results are all lying near to the trend predicted by the two-diode model.

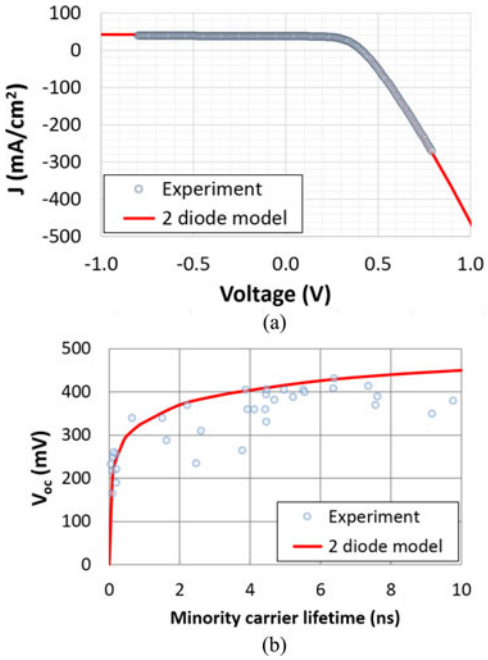

Fig. 8. (a) Illuminated *J–V* for the highest efficiency cell along with the calculations of the two diode model using the parameters in Table I. (b) Open-circuit voltage V_{oc} as a function of minority carrier lifetime for a series of different CZTSe-based solar cells along with a calculation extracted from the two-diode model using the parameters of Table I and varying the minority carrier lifetime.

It, therefore, seems that despite the presence of a large amount of potential fluctuations and band tail states in the absorber [19], [20], the current–voltage behavior of the solar cell is dominated by processes that can be well described with the standard two-diode model. In order to improve the V_{oc}, and thereby the device efficiency, the value of $J_{0,2}$ needs to be decreased. Taking into account (2), three possible pathways can be proposed to achieve this goal. The minority carrier lifetime could be strongly increased above the present value of 7 ns. This, of course, involves further passivation of defects in the absorber or at the different interfaces. At present, the minority carrier lifetime seems to be mainly limited by band tail states and a defect level with an activation energy of about 170 meV, as these are the defects that can be clearly measured with the different characterization methods. Unless a better fabrication procedure or a passivating material or element is found, the approach to increase the minority carrier lifetime seems difficult. A second approach would be to increase the acceptor density in the absorber in order to reduce the depletion region width. Nevertheless, carrier collection seems to be strongly relying on the internal electric field in the depletion region, as we usually see best carrier collection and highest short-circuit currents for the devices with the lowest doping in the absorber. This, therefore, might not be the best approach to obtain higher efficiencies. Finally, one could increase the bandgap. Through the exponential dependence of the intrinsic carrier density on the bandgap, the amount of recombination will also be strongly reduced. A small increase in the bandgap to about 1.2 eV already leads to a two order of magnitude lower recombination current with $J_{0.2} = 10^{-7}$ A/cm^2. As this can be achieved through introduction of a small percentage of sulfur in the absorber, this will probably be the preferred way to reduce the recombination currents in our devices.

V. Conclusion

We have characterized CZTSe–CdS–ZnO solar cells and investigated a series of nonidealities that are present in the devices. A barrier of about 300 meV at the absorber–buffer interface was derived, which is strongly reduced upon absorption of light in the CdS buffer layer; therefore, it does not represent a limitation for cell efficiency under standard AM1.5G illumination. A barrier at the backside contact of about 130 meV is also present, which could be reduced to 15 meV through the introduction of a thin TiN backside metal. Both barriers do only add a fraction of an $\Omega \cdot \text{cm}^2$ to the device series resistance; therefore, they do not limit the efficiency. Through comparison of the experimental current–voltage behavior with a two-diode model, using parameters extracted from electrooptical characterization, we can conclude that the efficiency of our devices is limited by strong recombination in the depletion region. The minority carrier lifetime is, therefore, limiting the open-circuit voltage of the device. Factors contributing to a low minority carrier lifetime of the order of 7 ns are likely band tail states caused by strong potential fluctuations and a defect measured from admittance spectroscopy with an activation energy of 170 meV. Further improvements to the CZTSe cells, as presented in this study, can be achieved by increasing the bandgap of the material and, thereby, reducing the amount of recombination in the depletion region; of course, this is only under the condition that all other device properties can be kept constant.

Acknowledgment

Hamamatsu photonics is acknowledged for providing the C12132 near-infrared compact fluorescence lifetime measurement system. AGC is acknowledged for providing SLG/Mo substrates.

References

[1] S. Siebentritt and S. Schorr, "Kesterites—A challenging material for solar cells," *Prog. Photovoltaic Res. Appl.*, vol. 20, no. 1, pp. 1–126, 2012.

[2] S. Delbos, "Kesterite thin films for photovoltaics: A review," *EPJ Photovoltaics*, vol. 3, pp. 35004-1–35004-13, 2012.

[3] W. Wang, M. T. Winkler, O. Gunawan, T. Gokmen, T. K. Todorov, Y. Zhu, and D. B. Mitzi, "Device characteristics of CZTSSe thin-film solar cells with 12.6% efficiency," *Adv. Energy Mater.*, vol. 4, no. 7, pp. 1301465-1–1301465-5, 2014.

[4] M. A. Green, K. Emery, Y. Hishikawa, and W. Warta, "Solar cell efficiency tables (version 37)," *Prog. Photovoltaic, Res. Appl.*, vol. 19, pp. 84–92, 2011.

[5] G. Brammertz, M. Buffière, S. Oueslati, H. El Anzeery, K. Ben Messaoud, S. Sahayaraj, C. Köble, M. Meuris, and J. Poortmans, "Characterization of defects in 9.7% efficient $Cu_2ZnSnSe_4$-CdS-ZnO solar cells," *Appl. Phys. Lett.*, vol. 103, pp. 163904-1–163904-4, 2013.

[6] G. Brammertz, Y. Ren, M. Buffière, S. Mertens, J. Hendrickx, H. Marko, A. E. Zaghi, N. Lenaers, C. Köble, J. Vleugels, M. Meuris, and J. Poortmans, "Electrical characterization of $Cu_2ZnSnSe_4$ solar cells from selenization of sputtered metal layers," *Thin Solid Films*, vol. 535, pp. 348–352, 2013.

[7] M. Grossberg, J. Krustok, J. Raudoja, K. Timmo, M. Altosaar, and T. Raadik, "Photoluminescence and Raman study of $Cu_2ZnSn(Se_xS_{1-x})_4$

monograins for photovoltaic applications," *Thin Solid Films*, vol. 519, pp. 7403–7406, 2011.

[8] A. Redinger, K. Hönes, X. Fontané, V. Izquierdo-Roca, E. Saucedo, N. Valle, A. Pérez-Rodríguez, and S. Siebentritt, "Detection of a ZnSe secondary phase in coevaporated $Cu_2ZnSnSe_4$ thin films," *Appl. Phys. Lett.*, vol. 98, pp. 101907-1–101907-3, 2011.

[9] M. Buffière, G. Brammertz, S. Oueslati, H. El Anzeery, J. Bekaert, K. Ben Messaoud, C. Köble, S. Khelifi, M. Meuris, and J. Poortmans, "Spectral current–voltage analysis of kesterite solar cells," *J. Phys. D, Appl. Phys.*, vol. 47, pp. 175101-1–175101-4, 2014.

[10] O. Gunawan, T. K. Todorov, and D. B. Mitzi, "Loss mechanisms in hydrazine-processed $Cu_2ZnSn(Se,S)_4$ solar cells," *Appl. Phys. Lett.*, vol. 97, pp. 233506-1–233506-4, 2010.

[11] S. Oueslati, H. El Anzeery, G. Brammertz, M. Buffière, O. ElDaif, O. Touayar, C. Köble, M. Meuris, and J. Poortmans, "Study of alternative back contacts for thin film $Cu_2ZnSnSe_4$-based solar cells," *J. Phys. D, Appl. Phys.*, 2013, submitted for publication.

[12] T. P. Weiss, A. Redinger, J. Luckas, M. Mousel, and S. Siebentritt, "Admittance spectroscopy in kesterite solar cells: Defect signal or circuit response," *Appl. Phys. Lett.*, vol. 102, pp. 202105-1–202105-4, 2013.

[13] T. Walter, R. Herbenholz, C. Mueller, and H. W. Schock, "Determination of defect distributions from admittance measurements and applications to $Cu(In,Ga)Se_2$ based heterojunctions," *J. Appl. Phys.*, vol. 80, pp. 4411–4420, 1996.

[14] T. Gokmen, O. Gunawan, and D. B. Mitzi, "Minority carrier diffusion length extraction in $Cu_2ZnSn(Se,S)_4$ solar cells," *Appl. Phys. Lett.*, vol. 114, pp. 114511-1–114511-4, 2013.

[15] X. X. Liu and J. R. Sites, "Solar cell efficiency and its variation with voltage," *J. Appl. Phys.*, vol. 75, no. 1, pp. 577–581, 1993.

[16] A. Luque and S. Hegedus, *Handbook of Photovoltaic Science and Engineering*. West Sussex, U.K.: Wiley, 2010, pp. 61–92.

[17] H.-R. Liu, S. Chen, Y.-T. Zhai, H. J. Xiang, X. G. Gong, and S.-H. Wei, "First-principles study on the effective masses of zinc-blend-derived Cu_2Zn $IVVI_4$ (IV = Sn, Ge, Si and VI = S, Se)," *J. Appl. Phys.*, vol. 112, pp. 093717-1–093717-6, 2012.

[18] O. Gunawan, T. Gokmen, C. W. Warren, J. D. Cohen, T. K. Todorov, D. A. R. Barkhouse, S. Bag, J. Tang, B. Shin, and D. B. Mitzi, "Electronic properties of the $Cu_2ZnSn(Se,S)_4$ absorber layer in solar cells as revealed by admittance spectroscopy and related methods," *Appl. Phys. Lett.*, vol. 100, pp. 253905-1–253905-4, 2012.

[19] T. Gokmen, O. Gunawan, T. K. Todorov, and D. B. Mitzi, "Band tailing and efficiency limitation in kesterite solar cells," *Appl. Phys. Lett.*, vol. 103, pp. 13506-1–12506-5, 2013.

[20] S. Oueslati, G. Brammertz, M. Buffiere, C. Köble, M. Meuris, T. Walid, and J. Poortmans, "Photoluminescence study and observation of unusual optical transitions in $ZnO/CdS/Cu_2ZnSnSe_4$ solar cells," *Solar Energy Mater. Solar Cells*, DOI: 10.1016/j.solmat.2014.10.041, 2015

Guy Brammertz received the M.S. degree in applied physics from the University of Liège, Liège, Belgium, in 1999 and the Ph.D. degree in applied physics from the University of Twente, Enschede, The Netherlands, in 2003.

In 2004, he joined IMEC, Diepenbeek, Belgium, where he was involved in the CMOS program, working on the development of III–V transistors. His main research interests include epitaxial growth of compound semiconductor layers and the passivation and electrical characterization of oxide–semiconductor interfaces. In 2011, he joined the IMEC Photovoltaics Department, where he started working on the fabrication and characterization of thin-film kesterite solar cells. In 2013, he joined IMOMEC, which is the associated laboratory of IMEC with Hasselt University, where he continued to focus his research activities on the development of thin-film photovoltaics. He authored and coauthored more than 100 scientific publications in technical journals.

Souhaib Oueslati received the B.S. degree in fundamental physics in 2010 and the M.Sc. degree in quantum physics from El Manar University, Tunis, Tunisia, in 2012.

From January 2013 to July 2014, he received a scholarship from King Abdul-Aziz City of Science and Technology (KACST)-Intel Consortium Center of Excellence in Nano-manufacturing Applications under the signed joint research and academic advising agreement between Intel Corporation, KACST, and ElManar University, Tunisia. The scholarship aims to complete his graduate studies (Ph.D.) as an international scholar registered with the Katholieke Universiteit Leuven and IMEC, Diepenbeek, Belgium. During the scholarship, he was a Researcher with the Alternative Thin Film Photo-Voltaic team, working on the solar cell processing of $Cu_2ZnSnSS(e)_4$ (CZTSSe) focusing on the electrical characterization and modeling of CZTSS(e) solar cells.

Marie Buffière received the M.S. degree in materials science from the University of Poitiers, Poitiers, France, in 2008 and the Ph.D. degree in materials science and electrical engineering from the University of Nantes, Nantes, France, in 2011.

In 2012, she joined IMEC, Leuven, Belgium, where she is currently a Postdoctoral Researcher with the PV Novel Materials group. Her main research interests include the fabrication of thin-film solar cells, the structural and electrical characterization of these devices, and the development of numerical models.

Jonas Bekaert received the M.S. degree in physics from the University of Antwerp, Antwerpen, Belgium, in 2014. He is currently working toward the Ph.D. degree with the University of Antwerp, where he works on a theoretical and computational study of multiband superconductors.

His experience with chalcogenide materials for photovoltaics mainly consists of a computational (*ab-initio*) study of native point defects and carbon-related impurities in $Cu(In,Ga)Se_2$. In addition to this, in 2013, he did an internship with IMEC, performing electrical characterization of $Cu_2ZnSn(S,Se)_4$ photovoltaic devices.

Hossam El Anzeery received the B.S. degree in instrumentation and control from the University of Technology Petronas, Teronoh, Malaysia, in 2010 and the M.Sc. degree in microelectronics system design from Nile University, Cairo, Egypt, in 2014.

From May 2010 to October 2011, he was an Engineer with Baker Hughes, Egypt. Between January 2013 and July 2014, he was a Researcher with the Alternative Thin Film Photo-Voltaic team, IMEC, Diepenbeek, Belgium, where he completed his Master's thesis on the optical characterization and optimization of thin-film absorber materials. He has worked with $Cu(In,Ga)Se_2$, $Cu_2ZnSnSe_4$, $Cu_2ZnGe(S,Se)_4$, and $Cu_2ZnSiSe_4$ absorbers. His current research interests include materials and devices for energy harvesting, especially inorganic solar cells and high-bandgap absorbers.

Khaled Ben Messaoud received the B.S. degree in physics and the M.Sc. degree in iron chalcogenide thin films from Tunis El Manar University, Tunis, Tunisia, in 2009 and 2011, respectively.

From 2007 to 2012, he was a Researcher with the unit of physics of semiconductor devices, specializing in the structural and optical properties of FeX_2 (X = S, Se and Te). From January 2013 to July 2014, he was part of the Alternative Thin Film Photo-Voltaic team (ATFPV), IMEC, Diepenbeek, Belgium, in collaboration with the Center of Excellence for Nanotechnology Applications, Riyadh, KSA, working on the solar cell processing of $Cu_2ZnSnSe_4$ (CZTSe) and $CuInGaSe_2$ (CIGSe) photovoltaic cells, focusing on the study of the CdS/CZTSe and CdS/CIGSe heterointerface as a part of his Ph.D. dissertation. His main research interests include materials and devices for absorber and buffer layers of thin-film solar cells and semiconductor devices.

Sylvester Sahayaraj, photograph and biography not available at the time of publication.

Thomas Nuytten received the Ph.D. degree in physics from the Katholieke Universiteit Leuven, Leuven, Belgium, in 2009.

He subsequently worked as a Postdoctoral Researcher in the field of semiconductor nanostructures and energy conversion systems. In 2013, he joined IMEC, Leuven, Belgium, as a Researcher, where his main interests include spectroscopic and electrical characterization of next-generation semiconductor technologies.

Christine Köble, photograph and biography not available at the time of publication.

Marc Meuris received the M.S. degree in physics and the Ph.D. degree in physics from the Katholieke Universiteit Leuven, Leuven, Belgium, in 1983 and 1990, respectively.

In 1984, he joined IMEC, Leuven. In the first year, he worked on RTP anneal process development of dopants in III–V material. Then, he transferred to the analysis group with IMEC, headed by W. Vandervorst, where he did his Ph.D. research on secondary ion-mass spectroscopy. From 1990 to 1999, he was within the group of M. Heyns on cleaning technology for improving the gate oxide integrity, resulting in the development of the IMEC Clean as a pregate and prediffusion clean for CMOS processing. From 1997 to 2002, he was the CMP Group Leader with IMEC. In 2002, he was the Technical Advisor of IMEC CMOS projects for collaborations with Flemish industry. In 2003, he became the Program Manager of the Ge program with IMEC. In 2006, this program enlarged its focus to Ge and III–V materials for scaling CMOS devices with high-mobility materials. In 2010, he became a Program Manager with the Photovoltaic Department of J. Poortmans to start up the PV Novel Materials team, which also includes CIGS and alternative inorganic materials for thin-film PV. In 2013, due to its focus on advanced material research, the team moved to IMOMEC (which is the associated laboratory of IMEC with Hasselt University). He has authored and coauthored more than 450 scientific publications and as an inventor holds more than 45 patents.

Jozef Poortmans received the degree in electronic engineering from the Katholieke Universiteit Leuven (KU Leuven), Leuven, Belgium, in 1985 and the Ph.D. degree in June 1993, also from KU Leuven.

He joined the newly build Interuniversitary Microelectronic Centre (IMEC), Leuven, where he worked on laser recrystallization of polysilicon and a-Si for SOI-applications and thin-film transistors. In 1988, he started his Ph.D. research on strained SiGe-layers. Both the deposition and the use of these SiGe alloys within the base of a heterojunction bipolar transistor were investigated in the frame of this study. Afterward, he joined the photovoltaics group, where he became responsible for the group Advanced Solar Cells. Within this frame, he started activity about thin-film crystalline Si solar cells with IMEC. He has coordinated several European Projects in this domain during the fourth and fifth European Framework Program. He is currently the Scientific Director of the PV activities with IMEC. As a Board Member of the EUREC agency and a member of the Steering Committee of the EU PV Technology Platform, he is involved in the preparation of the Strategic Research Agenda for Photovoltaic Solar Energy Technology of the European PV Technology Platform. He also acted as the General Chairman of the 21st European Photovoltaic Solar Energy Conference and Exhibition and of the SiliconPV 2012 Conference. He has authored or coauthored more than 500 papers that have been published in conference proceedings and technical journals. Since 2008, he is also been a part-time Professor with the Katholieke Universiteit Leuven, where he teaches courses on photovoltaics and materials in electrical engineering. Since 2013, he has also been a fellow with IMEC.